

are necessary and that LCO testing should continue to be performed by engineers well versed in classical flutter flight test procedures.

References

- 1 Norton, W. J., "Limit Cycle Oscillation and Flight Flutter Testing," *Proceedings of the 21st Annual Symposium*, Society of Flight Test Engineers, Lancaster, CA, 1990, pp. 3.4-1-3.4-12.
- 2 Cunningham, A. M., Jr., "Practical Problems: Airplanes," *Unsteady Transonic Aerodynamics*, AIAA, Washington, DC, 1989, Chap. 3, pp. 83, 84.
- 3 Denegri, C. M., Jr., "Limit Cycle Oscillation Flight Test Results of a Fighter with External Stores," *Journal of Aircraft*, Vol. 37, No. 5, 2000, pp. 761-769.
- 4 *Airplane Strength and Rigidity—Vibration, Flutter, and Divergence*, MIL-SPEC MIL-A-8870B, 20 May 1987, p. 3.
- 5 Dreyer, C. A., and Shoch, D. L., "F-16 Flutter Testing at Eglin Air Force Base," AIAA Paper 86-9819, April 1986.

Results of Theodorsen and Garrick Revisited

Thomas A. Zeiler*

University of Alabama, Tuscaloosa, Alabama 35487

Nomenclature

<i>a</i>	= distance, in semichords, between airfoil midchord and elastic axis (see Fig. 1)
<i>b</i>	= airfoil semichord
<i>h</i>	= airfoil plunge displacement (see Fig. 1)
<i>k</i>	= reduced frequency, $\omega b / V$
<i>m</i>	= airfoil mass (per unit span)
<i>r</i> _{<i>α</i>}	= radius of gyration, in semichords, of airfoil with respect to the elastic axis
<i>V</i>	= airspeed
<i>x</i> _{<i>α</i>}	= distance, in semichords, from airfoil elastic axis to center of mass (see Fig. 1)
<i>α</i>	= airfoil pitch displacement (see Fig. 1)
<i>μ</i>	= airfoil mass ratio, $m / \rho \pi b^2$
<i>ρ</i>	= air mass density
<i>ω</i> _{<i>h</i>}	= uncoupled plunge radian frequency
<i>ω</i> _{<i>α</i>}	= uncoupled pitch radian frequency

Introduction

DURING the first half of the 20th century, Theodore Theodorsen formulated the first analytically exact unsteady aerodynamic theory for modeling the mechanism of aeroelastic flutter.¹ The case considered was that of the two-dimensional airfoil section, with degrees of freedom in plunge, pitch, and trailing-edge control surface rotation, in unsteady, incompressible flow. Theodorsen with I. E. Garrick, authored several NACA reports^{2,3} containing plots of a critical flutter speed parameter for ranges of a variety of airfoil and flow parameters.

The airfoil flutter theory and results of Theodorsen and Garrick^{2,3} are likely no longer used by anyone for designing safe, operational vehicles, but they do serve useful purposes. The Theodorsen theory¹ is still a useful educational tool in universities, being the simplest flutter problem that students can prepare computer solutions for with relative ease and at the same time learn the essential character of solving flutter equations. In addition, the Theodorsen flutter

solution, being for two-dimensional, incompressible, inviscid flow, provides a limiting case for any newly developed computational fluid dynamics schemes. Although the theory is flawless, the computational resources available at the time (when computer was a job title!) leave much to be desired when compared to the resources available today. Some years ago, while doing his doctoral work, the present author found⁴ a number of erroneous plots in the reports of Theodorsen and Garrick^{2,3} and in other work that references their results.^{5,6} The amount of heartburn and time that the author spent checking and rechecking could have been saved had it been known that some (if not many, or all!) of the flutter boundaries in the old NACA reports and texts were in error. The same could be said of other research situations, and of the theory's use in the classroom.

It is evident that the errors in the original plots are not generally known. Certainly none of the author's dissertation committee knew, and none of them were ignorant people. The purpose of this Note is to ensure that the existence of the errors is generally known and to provide a few corrected plots to the community at large. One does not set about lightly to correct the masters, and only after numerous rederivations is there confidence that the results presented herein are correct.

Computational Results and Discussion

The standard *V-g* method of flutter analysis for the two-degree-of-freedom (2-DOF) airfoil, Fig. 1, was implemented in MATLAB.⁷ MATLAB's zooming feature was used to isolate the airspeed at the critical flutter point. Several plots of flutter boundaries from the literature are presented to illustrate the errors. In Figures 3, 4, and 5, BAH refers to Ref. 5, BA refers to Ref. 6, and T&G refers to Theodorsen and Garrick, either Ref. 2 or 3, specified in the text as needed.

Figure 2 shows a set of flutter boundaries vs frequency ratio for a set of values of *x*_{*α*}. The curves in Fig. 2 were obtained from Ref. 6 (they also appear in Ref. 5). For these curves, *a* = -0.3, *μ* = 20, and *r*_{*α*} = 0.5. For the lower values of the abscissa, there is agreement

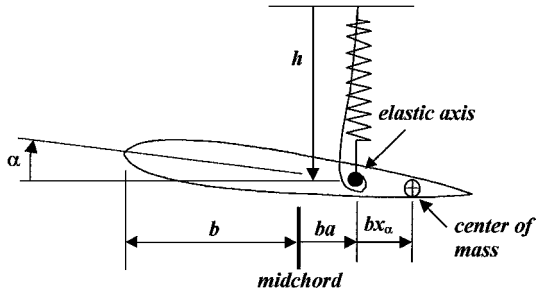


Fig. 1 Airfoil geometry, two-DOF.

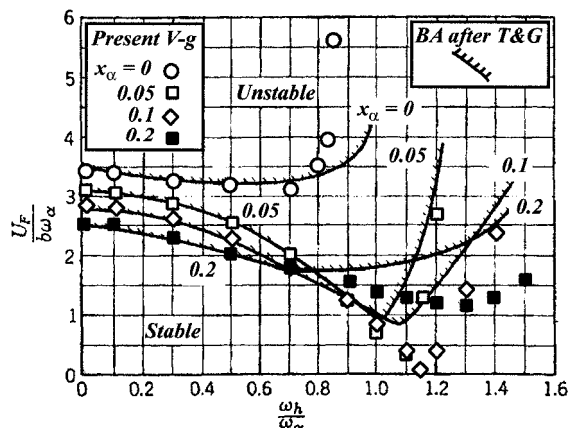


Fig. 2 First comparison of flutter boundaries from Refs. 2, 5, and 6 with present computations.

Received 22 May 1999; revision received 20 April 2000; accepted for publication 8 May 2000. Copyright © 2000 by the American Institute of Aeronautics and Astronautics, Inc. All rights reserved.

*Assistant Professor, Department of Aerospace Engineering and Mechanics, 205 Hardaway Hall, Box 870280. Senior Member AIAA.

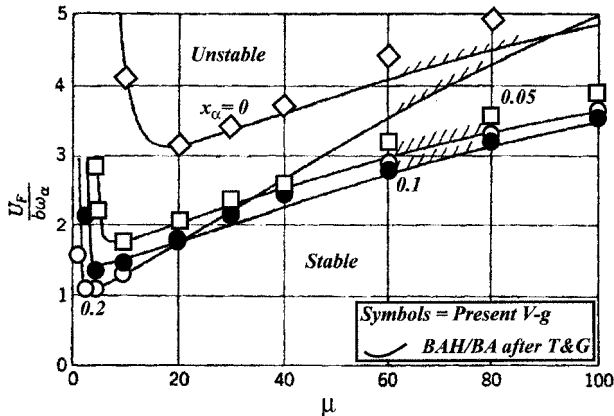


Fig. 3 Second comparison of flutter boundaries from Refs. 2, 5, and 6 with present computations.

between the original curves and the present computations. Also, though there are significant discrepancies in the values of the flutter parameter for higher values of frequency ratio, the general trends observed in the present calculations are consistent with those of the original plots.

Figure 3 shows a set of flutter boundaries vs the airfoil mass ratio for a set of values of x_α . These plots are interesting because they appear in Refs. 2 and 5 for the mass ratio varying only from zero to a value of 30. In Ref. 6, from where the curves in Fig. 3 were obtained, these plots appear with the mass ratio extending to 100. However, some of the curves are mislabeled (with the corresponding value of x_α) in Ref. 6. Furthermore, although the present computations agree with the original plots for the lower values of μ , there are again serious discrepancies at higher values. Because the corresponding curves in Ref. 6 are mislabeled to begin with, only the present computations (the symbols) are labeled in Fig. 3. In whatever fashion the curves in Ref. 6 were supposed to be labeled originally is quite irrelevant because they are incorrect anyway. These errors notwithstanding, the present computations still display the same general trends as the original curves, although the rise in flutter speed for $x_\alpha = 0.2$ as μ increases is not quite as dramatic as the erroneous curve suggests.

The final plot, Fig. 4, is taken directly from Ref. 4 and illustrates what is probably the most important reason that the present article was written. Figure 6 shows four separate computations of flutter boundaries for the three-DOF airfoil (that is, with trailing-edge control). References 47 and 48 in Fig. 4 correspond to the present article's Refs. 3 and 8. Also shown are flutter computations that incorporated a rational function approximation for the unsteady aerodynamics, as well as results using the $V-g$ method (labeled $U-g$). The hinge of the trailing-edge control (aileron) is at the 60% chord. The radius of gyration in semichords of the aileron with respect to the hinge, referenced to the total mass of the airfoil, is 0.002. The location of the aileron c.m. with respect to the hinge line multiplied by the ratio of the aileron mass to the total airfoil mass is 0.002. Also, $(\omega_h/\omega_\alpha) = 0.607$, $a = -0.2$, $\mu = 12$, and $r_\alpha = 0.25$. Flutter boundaries are plotted vs the ratio of the uncoupled aileron frequency and the uncoupled pitch (or torsion) frequency.

Clearly, the two methods from Ref. 4 and the computation done in Ref. 8 agree with one another better than they do the original plots from Ref. 3. What makes this plot important is that the computations done in Ref. 8 were for a transonic flow theory that was being tested for a low (incompressible) Mach number case, but the author of Ref. 8 and his advisor (who was on this author's committee) were at a loss to explain the discrepancy. This experience shows that testing of any new theory or computer code for unsteady aeroelastic modeling and analysis that uses the incompressible two-dimensional airfoil results of Theodorsen and Garrick^{2,3} for check cases should not rely upon the plots that appear in Refs. 1–3, or in Refs. 5 and 6. Note that the several flutter calculations (for zero structural damping) found in Fung's text⁹ agree with calculations done by the present author.

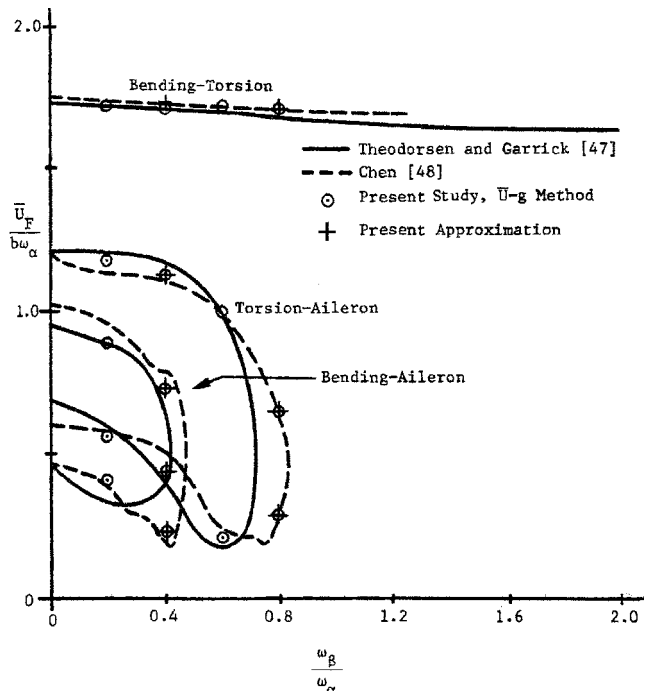


Fig. 4 Comparison of three-DOF airfoil flutter boundaries reproduced from Ref. 4.

Summary, Conclusions, and Recommendations

Evidence is presented in this article that some of the flutter boundaries (for the two- and three-DOF, two-dimensional airfoil in incompressible, inviscid flow) found in the NACA reports by Theodorsen and Garrick^{2,3} are in error, and that many others might also be in error. Furthermore some of the erroneous plots have found their way into some classic texts on aeroelasticity. It is suspected that the state of computational capabilities that existed at the time the original NACA reports were prepared contributed in large measure to the errors. The exact errors made have not been identified, however, and may never be. It is a comment on how far computational capabilities have developed to note that today's undergraduate student, with a little tutoring, should be capable of performing these computations with a speed and accuracy once unimaginable.

The present author has not recomputed all of the plots found in the NACA reports by Theodorsen and Garrick,^{2,3} and does not suspect that any new insights or old misconceptions will be revealed by doing so. Nonetheless, it is recommended that all of the plots in these classic and historically important NACA documents be recomputed and published. Such an undertaking would serve two purposes: it would provide numerically correct results for others to use as check cases, and it would bring a sense of closure to the groundbreaking work done by Theodore Theodorsen and I. E. Garrick.

References

- Theodorsen, T., "General Theory of Aerodynamic Instability and the Mechanism of Flutter," NACA TR-629, May 1934.
- Theodorsen, T., and Garrick, I. E., "Mechanism of Flutter, a Theoretical and Experimental Investigation of the Flutter Problem," NACA TR-685, Sept. 1938.
- Theodorsen, T., and Garrick, I. E., "Flutter Calculations in Three Degrees of Freedom," NACA TR-741, June 1941.
- Zeiler, T. A., "An Approach to Integrated Aeropropulsive Tailoring for Stability," Ph.D. Dissertation, School of Aeronautics and Astronautics, Purdue Univ., Lafayette, IN, Aug. 1985.
- Bisplinghoff, R. L., Ashley, H., and Halfman, R. L., *Aeroelasticity*, Addison Wesley Longman, Reading, MA, 1955, p. 540.
- Bisplinghoff, R. L., and Ashley, H., *Principles of Aeroelasticity*, Dover, New York, 1975, pp. 247, 248.
- "MATLAB: Using MATLAB Version 5," The MathWorks, Inc., Natick, Massachusetts, 1998.

⁸Chen, C.-H., "Flutter and Time Response Analyses of Three Degrees of Freedom Airfoils in Transonic Flow," Ph.D. Dissertation, School of Aeronautics and Astronautics, Purdue Univ., Lafayette, IN, Aug. 1981.

⁹Fung, Y. C., *An Introduction to the Theory of Aeroelasticity*, Dover, New York, 1993, pp. 224, 238.

Flow Complexities of Slender Wing Rock

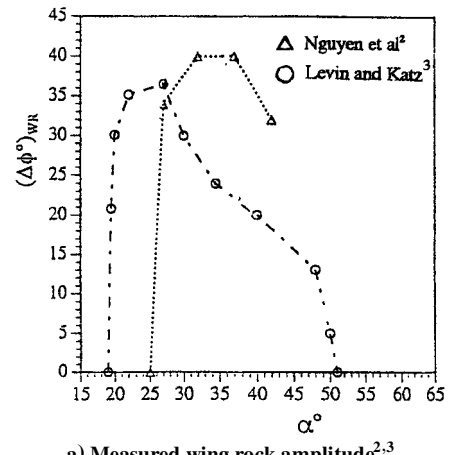
Lars E. Ericsson*
Mountain View, California 94040

Introduction

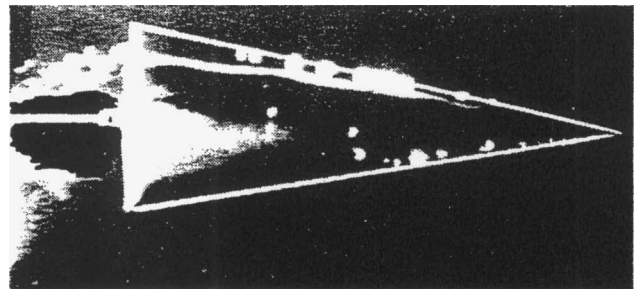
MILITARY design trends toward the use of unmanned, finless aircraft¹ have renewed interest in the unsteady aerodynamics of slender wing rock. One important aspect of the problem of wing rock control is the potential impact of typical configurational details on delta-wing aircraft, such as the presence of a centerbody. Early experimental results for a sharp-edged 80-deg delta wing indicated that breakdown of the leading-edge vortices played a role^{2,3} (Fig. 1). It could be shown that rather than being the cause of the wing rock problem, the breakdown phenomenon limited the growth of the limit-cycle amplitude.⁴ By the consideration of the effect of the roll-induced sideslip on the effective leading-edge sweep of the windward (dipping) wing-half, an upper limit for the limit-cycle amplitude could be determined.^{5,6} The measured start of wing rock (Fig. 1a) is in good agreement with the prediction⁷ that, for zero bearing friction, loss of roll damping should occur at $\alpha \geq 20$ deg (Fig. 2). Bearing friction caused the delay to $\alpha = 25$ deg of the loss of roll damping in the test of a pure delta-wing model³ (Fig. 1a). It will be shown that the earlier start of wing rock for the other model³ was caused by the presence of a centerbody or fuselage.

As even unmanned combat aircraft are likely to have a fuselage or centerbody of some kind, it is important to know that the effect of a centerbody on delta-wing aerodynamics can be large.⁸ Experimental results for a 69.33-deg delta-wing-body configuration demonstrated that the centerbody promoted vortex breakdown.⁹ This could be explained by the body-induced camber effect,^{8,10} which according to experimental results for the effect of static camber,¹¹ would have promoted breakdown, in agreement with the experimental results. Figure 3 shows configurational details of the models giving the results in Fig. 1. Whereas the Langley model² behaves essentially as a pure, sharp-edged delta wing, the other model³ has a centerbody. Because of its bluntness,¹² it behaves as a cylindrical centerbody,^{9,10} promoting vortex breakdown, thereby causing a reduction of the maximum wing rock amplitude. The earlier loss of roll damping, before the predicted value⁷ $\alpha \approx 20$ deg (Fig. 2), could also have been caused by the presence of the centerbody. By limiting the wing area, the centerbody acts to increase the effective leading-edge sweep, thereby causing earlier loss of roll damping.

The experimental results¹³ in Fig. 4 show that when a pointed ogive-cylinder centerbody, similar to the one used in Ref. 9, is moved aft to start behind the wing apex, as in the case of the extensively tested 65-deg delta-wing-body configuration,¹³ instead of promoting breakdown, the body delayed vortex breakdown to occur 30% or more aft of the measured position for a pure 65-deg delta-wing.¹⁴ It is described in Ref. 5 how this is the expected result when the pointed ogive-cylinder body is moved aft, as shown in Fig. 4,



a) Measured wing rock amplitude^{2,3}



b) Flow visualization of vortex breakdown at σ = 25 deg (Ref. 3)

Fig. 1 Wing rock of 80-deg delta wing.

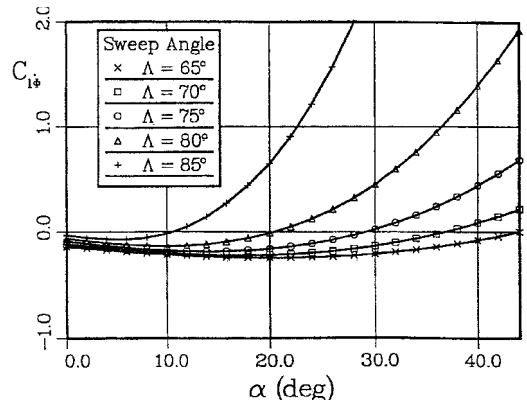


Fig. 2 Effect of leading-edge sweep on delta wing roll damping.⁷

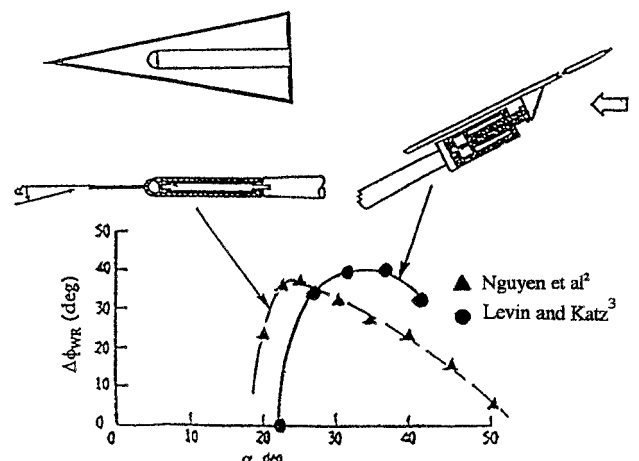


Fig. 3 Effect on wing rock results of geometric details of the test model.^{2,3}

Presented as Paper 99-0141 at the 37th Aerospace Sciences Meeting, Reno, NV, 11-14 January 1999; received 15 February 1999; accepted for publication 13 April 2000. Copyright © 2000 by Lars E. Ericsson. Published by the American Institute of Aeronautics and Astronautics, Inc., with permission.

*Consulting Engineer. Fellow AIAA.